

# Muon radiography technology for detecting high- $Z$ materials<sup>\*</sup>

MA Ling-Ling(马玲玲) WANG Wen-Xin(王文昕) ZHOU Jian-Rong(周建荣)  
SUN Shao-Hua(孙少华) LIU Zuo-Ye(刘作业) LI Lu(李露)  
DU Hong-Chuan(杜洪川) ZHANG Xiao-Dong(张小东) HU Bi-Tao(胡碧涛)<sup>1)</sup>

School of Nuclear Science and Technology, Lanzhou University, Lanzhou 730000, China

**Abstract** This paper studies the possibility of using the scattering of cosmic muons to identify threatening high- $Z$  materials. Various scenarios of threat material detection are simulated with the Geant4 toolkit. PoCA (Point of Closest Approach) algorithm reconstructing muon track gives 3D radiography images of the target material.  $Z$ -discrimination capability, effects of the placement of high- $Z$  materials, shielding materials inside the cargo, and spatial resolution of position sensitive detector for muon radiography are carefully studied. Our results show that a detector position resolution of 50  $\mu\text{m}$  is good enough for shielded materials detection.

**Key words** cosmic ray muons, muon radiography, PoCA algorithm, high- $Z$  materials, multiple scattering

**PACS** 24.10.Lx, 25.30.Mr, 25.80Dj

## 1 Introduction

Multi-energy tomography can simultaneously determine the density and the effective atomic number of each volume element. But CAT-scanning (Computerized Axial Tomography) of large volumes is very challenging (the largest CAT systems have only a one meter aperture). The energy of the X-rays must be increased significantly for penetrating an adequate depth and the total flux of photons delivered to the container also has to be increased significantly in order to keep the scan duration in a reasonable time. These specialized CAT-scanners would require both a massive shielding to protect the operator and enormous power sources.

One claims the pulsed fast neutron analysis to be material specific, not dependent on operator skill, and hard to make mistake. Most of these claims are based on laboratory detection of conventional high explosives or drugs among low density materials such as textiles. While fast neutrons can penetrate tile and excite shielded nuclear materials to emit a characteristic gamma ray, there are some questions concerning whether the detected gammas will retain their energy

“fingerprint” due to absorption and scattering. Just as in the case of passive detection, a determined terrorist can fill a void with material to absorb and/or scatter all of the gamma rays, effectively disabling all of the current inspection technologies.

The MU-Vision MU-detector is designed to detect and locate dense materials and voids in X-ray impervious, homogenous cargos by taking advantage of natural cosmic-ray-produced muons with a mean energy of 3–4 GeV at sea level. When the muons pass through an object, their trajectory is affected by coulomb scattering from the atoms in the material. Conceptually, to identify a nuclear weapon hidden in a cargo container, one could measure the incoming and outgoing directions of the muons. The denser materials and those with higher  $Z$  causing more deflection in the trajectories make cosmic muons a promising technique and an attractive ideal [1] for high- $Z$  material detection such as uranium.

In this paper, muons “generated” by the Geant4 toolkit with the distribution of energies and angles corresponding to cosmic ray muons at sea level propagate through a test volume to understand the discrimination of the low- $Z$  materials, medium- $Z$  materials,

---

Received 15 May 2009

<sup>\*</sup> Supported by National Natural Science Foundation of China (10575046,10775062) and Program for New Century Excellent Talents in University

1) E-mail: hubt@lzu.edu.cn

©2009 Chinese Physical Society and the Institute of High Energy Physics of the Chinese Academy of Sciences and the Institute of Modern Physics of the Chinese Academy of Sciences and IOP Publishing Ltd

high- $Z$  materials via a simple example. Especially, this work focused on the study of the effects of spatial resolution of a position sensitive detector for muon radiography without specifying the detector itself. Reconstruction of different scenarios of threat material and the different reconstruction methods need different spatial resolution of detector.

## 2 Monte Carlo simulations

The geometry of the muon radiography experimental apparatus simulated here is shown in Fig. 1. The apparatus consists of four horizontal position-sensitive detectors. The muons pass through the top two detectors, providing the incoming angle and position, then they pass through the object volume and are scattered. The bottom two detectors measure the positions and angles of the scattered particles. Each detector measures the particle position in  $x$  and  $y$  locations. Further, the scattering points and the scattering angles  $\theta$  are calculated.

The Geant4 toolkit simulates the interaction when the muons pass through the material. The simulated cosmic muon flux is generated in front of the top detectors with randomized starting positions and incident angles. The energy spectrum of the muons is based on cosmic ray muons at sea level [2–4]. The incident angular distribution is generated as  $\cos^2 \theta$ , where  $\theta$  is the plane angle from vertical [6]. The muon flux reaching the surface of the Earth is about 10000 per minute per square meter [5], Geant4 simulated the passage of about 100000 muons through the objects in this paper.

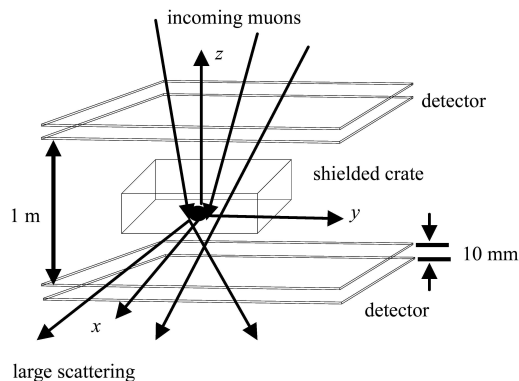


Fig. 1. The conceptual sketch of the simulated experimental setup. The size of the detectors is  $2\text{ m} \times 2\text{ m} \times 1\text{ mm}$ .

In this paper, we just used a plane replace the detector in order to investigate how well this technique works for detecting nuclear materials. The spatial resolution of the detectors is simulated in Geant4 by

smearing the position coordinates at the detector in the  $x$  and  $y$  directions with a Gaussian shape random number generator, with a standard deviation of 50, 100, 200  $\mu\text{m}$ .

## 3 Image reconstruction algorithm

Muon radiography needs to use the information from multiple Coulomb scattering. High energy muons passing through a material are deflected by nuclei and electrons of the material. As a result of multiple scattering, the muon passes through the material on a stochastic path. The muon emerges from material with an aggregate scattered angle  $\theta$  [5].

The PoCA (Point of Closest Approach) method is the muon radiography algorithm. [5, 6] In the PoCA reconstruction algorithm the incoming and the outgoing tracks of the muon are regarded as straight lines and the scattering is assumed to take place only once on a single point. The single scattering point is considered as the closest point to the incoming and the outgoing tracks of the muon, which is the so-called the “PoCA point”. We can get muon radiography by plotting the reconstructed PoCA points.

To improve the quality of the muon radiography over the plotting of raw PoCA points, we used voxels to get the reconstruction image [7]. In this method, the detector volume with 2 m in length, 2 m in width and 1 m in height, as shown in Fig.1, is divided into 4000000 smaller voxels ( $1\text{ cm} \times 1\text{ cm} \times 1\text{ cm}$ ). We took the sum of scattering angles of the PoCA points in a voxel and divided it by the number of PoCA points in that voxel to calculate the mean scattering angle for all voxels. The mean scattering angle is proportional to the  $z$  value of the material [5]. To get the reconstruction image, we plot the center point of each voxel and find that the pixel of the image is incremented in the case weighted with the mean scattering angle.

## 4 Simulation results and discussion

When muons pass through material, we use the PoCA method to get the PoCA points, and then reconstruct the image by plotting this raw PoCA points or using voxels. The dependence of muon radiography on different position resolutions of the detector is studied. The reconstruction is performed by the analysis tool of Matlab.

### 4.1 Results for a simple target scenario

We choose a test scene containing four  $5\text{ cm} \times 5\text{ cm} \times 5\text{ cm}$  blocks, made from U, Pb, Fe and Al placed at different positions. The abscissa of U, Pb,

Fe and Al is 10 cm,  $-30$  cm, 30 cm and  $-10$  cm, respectively. Fig. 2 shows the image reconstruction of the PoCA points with different position resolutions of  $0 \mu\text{m}$ ,  $50 \mu\text{m}$ ,  $100 \mu\text{m}$  and  $200 \mu\text{m}$ . The image gets worse as the with decreasing detector resolution.

With  $50 \mu\text{m}$  and  $100 \mu\text{m}$  resolution the targets are visible, whereas with  $200 \mu\text{m}$  resolution the shapes cannot be clearly recognized anymore. The corresponding created 2D histogram is histograms are shown in Fig. 3.

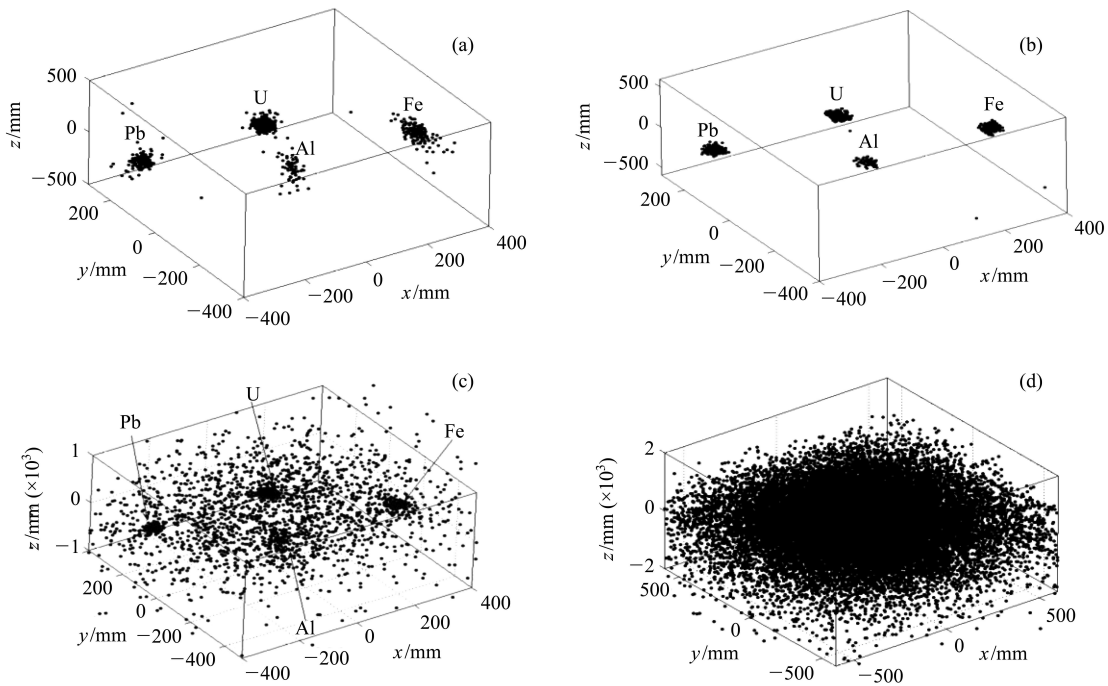


Fig. 2. Reconstruction image of the four blocks  $5 \text{ cm} \times 5 \text{ cm} \times 5 \text{ cm}$ , made of U, Pb, Fe, Al, and with detector resolutions are of  $0 \mu\text{m}$  (a),  $50 \mu\text{m}$  (b),  $100 \mu\text{m}$  (c) and  $200 \mu\text{m}$  (d), respectively.

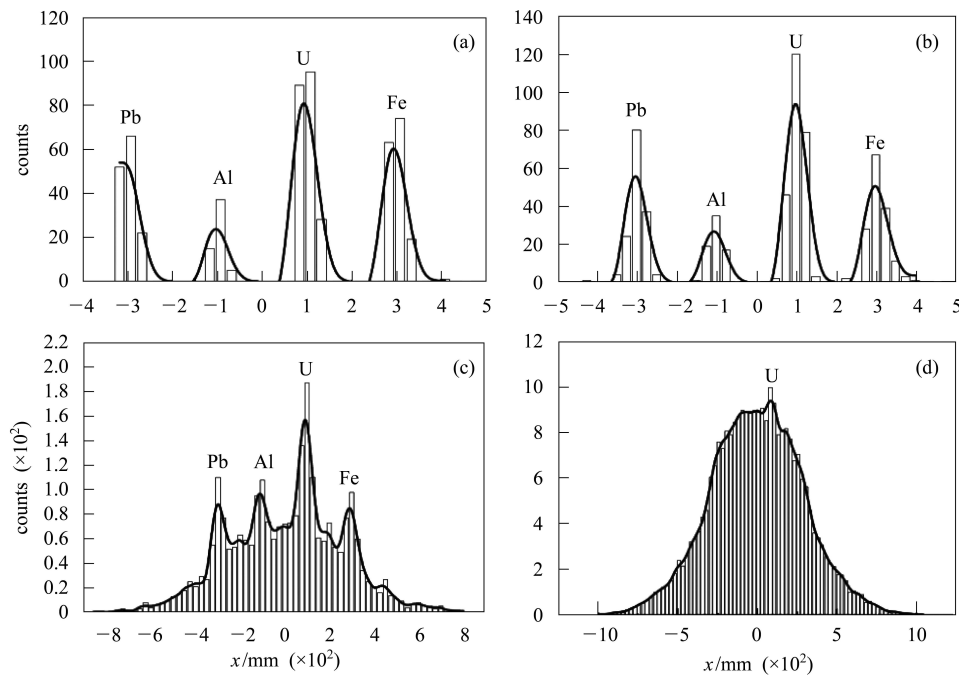


Fig. 3. The 2D histogram of all abscissa of every PoCA points, and with the detector resolutions are of  $0 \mu\text{m}$  (a),  $50 \mu\text{m}$  (b),  $100 \mu\text{m}$  (c) and  $200 \mu\text{m}$  (d), respectively.

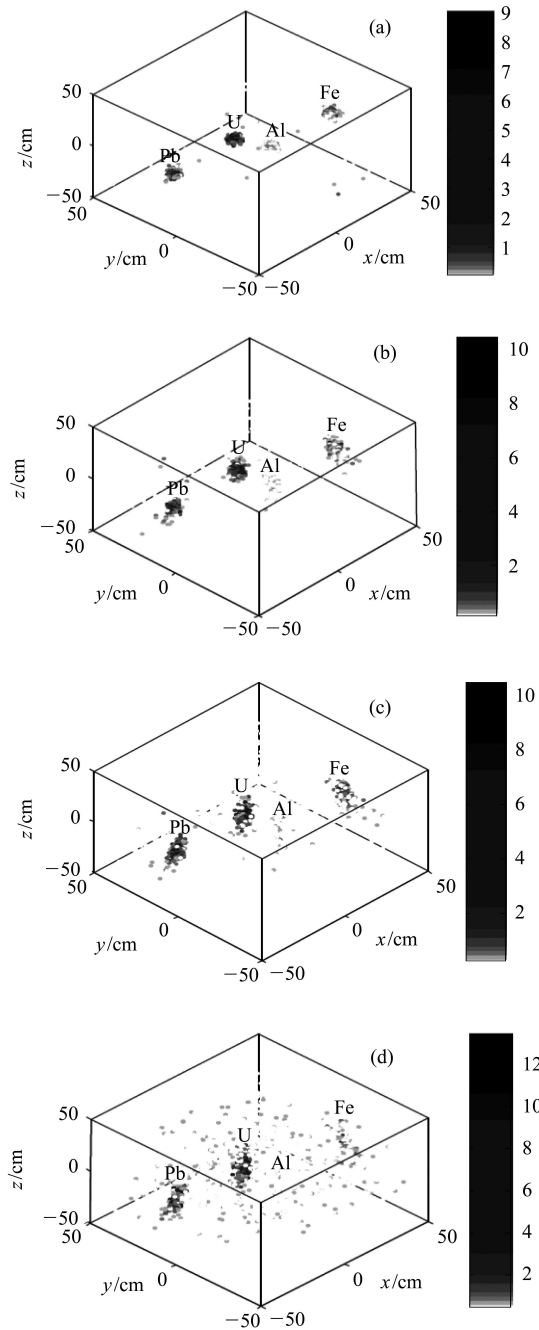


Fig. 4. The pixels of the reconstruction image are incremented, in the case weighted with the scattering angle  $\theta$ . Detector resolutions are 0  $\mu\text{m}$  (a), 50  $\mu\text{m}$  (b), 100  $\mu\text{m}$  (c) and 200  $\mu\text{m}$  (d), respectively.

U and Pb are high Z materials, Fe is a medium Z material, and Al is a low Z material. We can not get sufficient information from the image shown in Fig. 2 to discriminate the material Z between the Z values of the various materials because they have the same pixels. From the 2D histogram shown in Fig. 3, we might be able to discriminate between the materials through the counts of the PoCA points because the high-Z material has more materials have a higher

counts of PoCA points than low-Z materials.

Then we used voxels instead of plotting of the raw PoCA points to get a reconstruction image of the test scene. The image is shown in Fig. 4. Through this image the materials with different atomic numbers can be discriminated. The image gets worse as the detector resolution worsens, but with 50  $\mu\text{m}$ , 100  $\mu\text{m}$  and 200  $\mu\text{m}$  resolution the targets are visible. The shape of Al looks very vague with 200  $\mu\text{m}$  resolution.

#### 4.2 Results for the shielded targets scenario

In a realistic scenario, dense high-Z materials, for instance the spent nuclear fuel are located either in cargo containers or in shipping containers. The containers and shielding materials are usually iron. So we have made the simulation work according to the

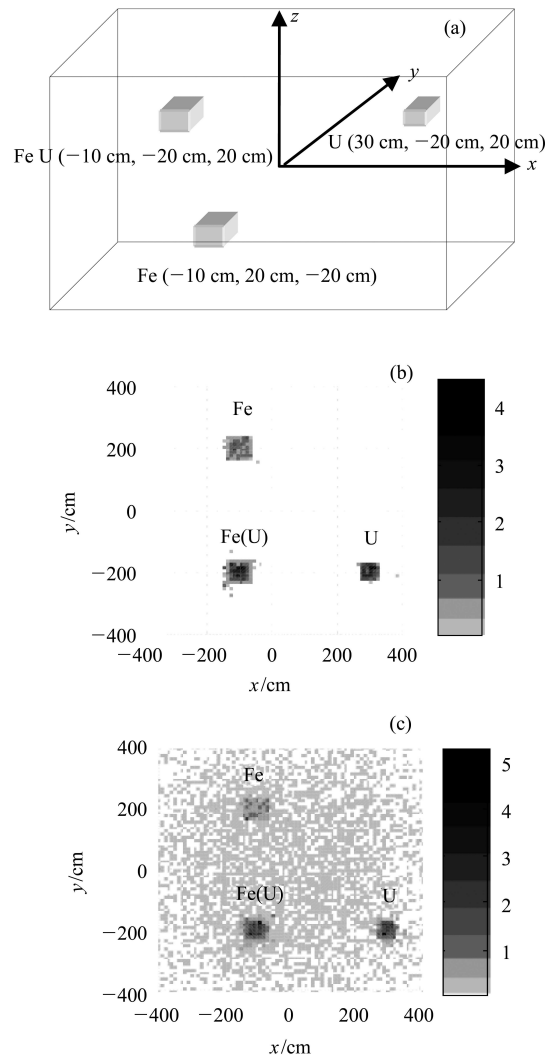


Fig. 5. (a) The geometry of the shielded target scenario. (b) Reconstruction image with the detector resolutions of 0  $\mu\text{m}$ . (c) Reconstruction image with the detector resolutions of 50  $\mu\text{m}$ .

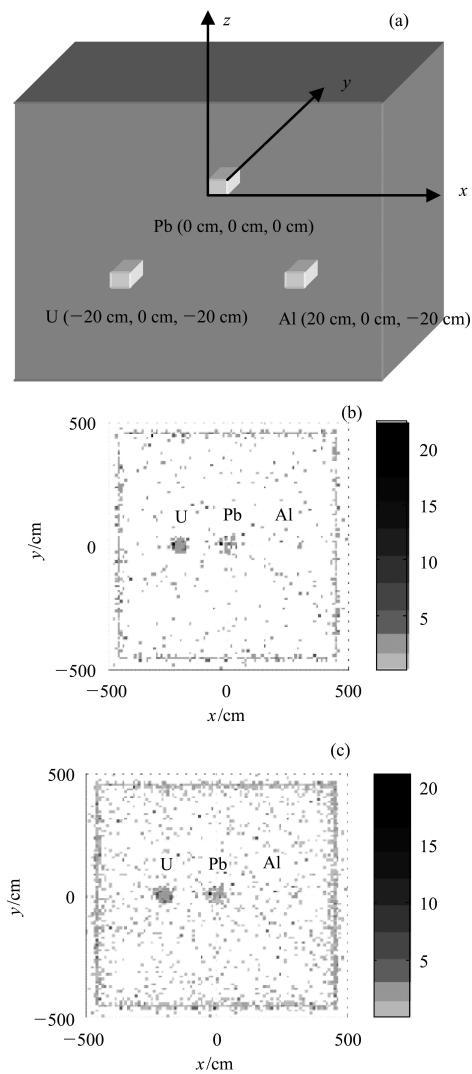


Fig. 6. (a) The geometry of the shielded target scenario. (b) Reconstruction result with the detector resolutions of  $0\ \mu\text{m}$ . (c) Reconstruction result with the detector resolution of  $50\ \mu\text{m}$ .

realistic scenario. In this section we provide the reconstruction image with detector resolution of  $50\ \mu\text{m}$  which is the best resolution for our resulting images.

The geometry of the shielded target scenario is shown in Fig. 5(a). The test sense arrangement contains three blocks, which are namely two U cores and

one Fe block. The two U cores have the same size of  $5\ \text{cm} \times 5\ \text{cm} \times 10\ \text{cm}$ , but one of them is shielded on each of its six sides by the lower  $Z$  material Fe with  $1\ \text{cm}$  in thickness. The size of the Fe block is  $7\ \text{cm} \times 7\ \text{cm} \times 12\ \text{cm}$ .

We used voxels in order to get the reconstruction results for the entire volume in a 2D top view. The reconstruction results shown in Fig. 5(b, c) demonstrate that the uranium cores can be distinguished from both shielding materials Fe with a detector resolution  $50\ \mu\text{m}$ . The U core is shown in dark, and shielded the low  $Z$  shielding material Fe is shown light in grey tone.

Another shielded target scenario is shown in Fig. 6(a). The geometry is that a big size ( $92\ \text{cm} \times 92\ \text{cm} \times 92\ \text{cm}$ ) Fe container with a  $1\ \text{cm}$  thick wall as the shielding material, and in the container we put three different  $Z$  materials U, Pb and Al with the same size of  $6\ \text{cm} \times 6\ \text{cm} \times 6\ \text{cm}$ . The purpose of simulating this shielded targets scenario, we target scenario was to investigate how to detect the dense high- $Z$  materials which are located either in cargo containers or in shipping containers.

The reconstruction results are shown in Fig. 6(b,c) and clearly give reproduce the outline of the geometry shown in Fig. 6(a). In this image the Al core is not very good visible but the high- $Z$  materials U and Pb are shown clearly, and we can distinguish them because the pixel of U is darker than that of Pb.

## 5 Conclusions

The results of the simulation presented in this paper indicate that it is indeed possible to distinguish materials with different  $Z$  using cosmic muon rays and that a high position resolution detector is necessary for the discrimination of high  $Z$  materials from the medium and low  $Z$  materials shielded by iron. To distinguish targets with no shielding material, a  $100\ \mu\text{m}$  detector resolution is enough. In all other cases a better detection resolution or better reconstruction method is needed.

## References

- Borozdin Konstantin N, Hogan Gary E. Christopher Morris et al. *Nature*, 2003, **422**: 277
- Nagamine K, Iwasaki M, Shimomura K et al. *Nucl. Instrum. Methods A*, 1995, **356**: 585
- Tanaka H K M, Nagamine K, Nakamura S N et al. *Nucl. Instrum. Methods A*, 2005, **555**: 164
- Tanaka H K M, Nakano T, Takahashi S et al. *Nucl. Instrum. Methods A*, 2007, **575**: 489
- Schultz L J, Borozdin K N, Gomez J J et al. *Nucl. Instrum. Methods A*, 2004, **519**: 687
- Joel Gustafsson. Tomography of Canisters for Spent Nuclear Fuel Using Cosmic-Ray Muons. In: Källne J. Uppsala University Neutron Physics Report. Sweden: Uppsala University, 2005
- <http://arxiv.org/pdf/0811.0187>